Hocine TILIOUINE

Gdansk Technical University Faculty of Electrical and Control Engineering

Comparative study of neural networks used in modeling and control of dynamic systems

Abstract: *In this paper, a diagonal recurrent neural network that contains two recurrent weights in the hidden layer is proposed for the designing of a synchronous generator control system. To demonstrate the superiority of the proposed neural network, a comparative study of performances, with two other neural networks, has been made. The investigated neural networks were: a feedforward neural network (FFNN), a first-order diagonal recurrent neural network (1_DRNN) and the proposed second-order diagonal recurrent neural network (2_DRNN). Moreover, to confirm the superiority of the proposed 2_DRNN, the results obtained with this network were also compared with those of the IEEE recommended conventional excitation control system (CECS).*

Streszczenie: *W artykule przedstawiono diagonalną rekurencyjną sieć neuronową do projektowania układu regulacji generatora synchronicznego. Proponowana sieć posiada dwie rekurencyjne wagi w warstwie ukrytej. Aby wykazać wyższość proponowanej sieci dokonano analizy porównawczej efektywności z dwoma innymi sieciami neuronowymi. Badanymi sieciami neuronowymi były: jednokierunkowa sieć neuronowa (FFNN), diagonalna rekurencyjna sieć neuronowa pierwszego rzędu (1_DRNN) oraz proponowana diagonalna rekurencyjna sieć neuronowa drugiego rzędu (2_DRNN). Ponadto, aby potwierdzić wyższość proponowanej sieci (2_DRNN), uzyskane wyniki dla tej sieci porównano z wynikami uzyskanymi dla konwencjonalnego układu regulacji (CECS) zalecanego przez IEEE. (**Studium porównawcze sieci neuronowych używanych w modelowaniu i sterowaniu systemami dynamicznymi**)*

Keywords: feedforward neural network, diagonal recurrent neural network, neurocontrol, turbogenerator.
Słowa kluczowe: sieci neuronowe, modelowanie.

Introduction

In the last three decades various neural network architectures have been used in modeling and control of dynamic systems [1÷16]. In most of these works feedforward neural network (FFNN), combined with tapped delays and using backpropagation algorithm for weight adaptation have been used successfully [1÷11]. However, the FFNN is a static network and without tapped delays it does not represent a dynamic system mapping. On the other hand, the recurrent neural network (RNN) has advantages that FFNN does not possess [12÷16]. Among these advantages we can mention the ability to store information for later use. Therefore the RNN is more suitable for dynamical systems than the FFNN. In this paper, diagonal recurrent neural networks (DRNN) are used to form the neuro-identifier (NI), which provides information about the plant to be controlled, and the neuro-controller (NC), which provides the necessary control signal to the plant. The DRNN can be made equivalent to a fully connected recurrent neural network (FCRNN). Contrary to FCRNN, in the DRNN there is no links between neurons in the hidden layer. Therefore, the DRNN has fewer weights than the FCRNN and shorter training time.

The paper is organized as follows. In the section II, a neural network based excitation control system is presented. In the section III, the training process for the considered neural networks is described. In the section IV, a generalized dynamic backpropagation algorithm (GDBPA) used in the training process is developed. In this same section are presented the structures of the studied neural networks: FFNN, first-order DRNN and second-order DRNN. In the section V, simulation tests are described and the results are illustrated and discussed. Finally, section VI gives the conclusion of the paper.

Neural network based excitation control system

The block diagram of the investigated neural network based excitation control system is shown in figure 1. It consists of two subnetworks: the first network, named neuro-identifier (NI), provides information about the plant to be controlled and the second, named neuro-controller (NC), provides the necessary control signal to the plant such that the error between plant and desired output is minimized.

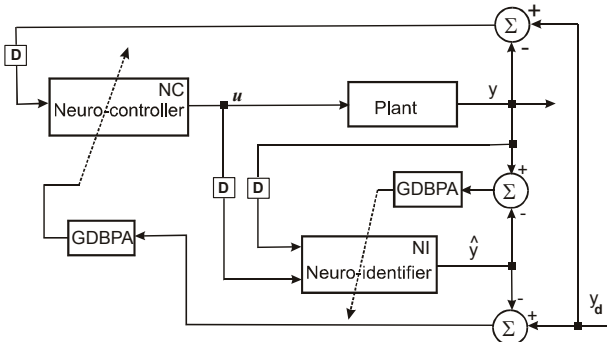

Fig. 1. Block diagram of neural network based excitation control system

The NI is a two-layered neural network with nine inputs: three delayed signals of the terminal voltage deviation (U_{ref}-U_g), three delayed signals of the active power deviation (P_{ref}-P_g) and three delayed signals of the controller output signal u. The hidden layer contains twelve neurons . The output layer has two neurons whose output are the predicted value U_g^* of terminal voltage and the predicted P_g^* of generator active power.

The NC is also a two-layered neural network with just six inputs: three delayed signals of the terminal voltage deviation (U_{ref}-U_g), three delayed signals of the active power deviation (P_{ref}-P_g). In the case of a feedforward neural network the hidden layer contains nine neurons and in the case of diagonal recurrent neural network six recurrent neurons. The NC output layer has one simple neuron whose output u provides the signal for the generator's excitation control.

The proposed controller 2_DRNN must ensure two functions: the function of an automatic voltage regulator (AVR) to maintain terminal voltage at the desired value U_{ref}, and the function of a power system stabilizer (PSS) for damping electromechanical oscillations. Therefore, its input signals are the voltage deviation and the active power deviation. The inputs of the two subnetworks NI and NC are time delayed by the sample period of 20 ms to create dynamic properties of the plant. For each input actual value and two previously delayed values are considered.

All neurons of both subnetworks NI and NC, with the exception of those in output layers, are nonlinear with the sigmoidal activation function:

$$\sigma(x) = \frac{1}{1+e^{-\beta x}} \tag{1}$$

where x represents the sum of the neuron input signals and β is the activation gain and has a constant value. The internal structures of the used neurons are given in figures 2, 3 and 4.

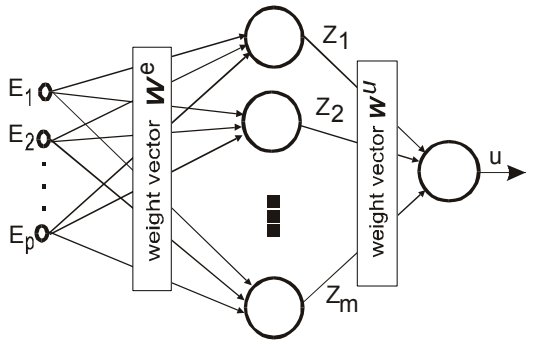

Fig. 2. Feedforward neural network structure

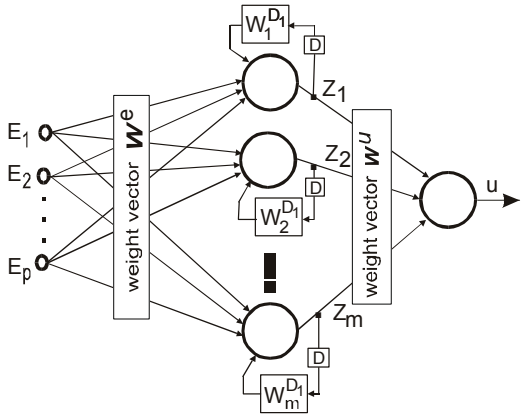

Fig. 3. First-order diagonal recurrent neural network structure

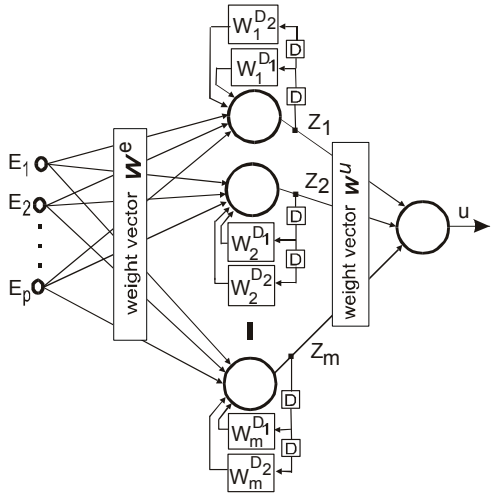

Fig. 4. Second-order diagonal recurrent neural network structure

The number of neurons in the hidden layers for both NI and NC are determined by using trial and error method. There is no theoretical considerations that can help to establish this parameter. Moreover, for the study of the transient stability there is no need to consider more than one hidden layer for both NI and NC. Nor, there is no need to consider more than three time delays for input signals [9].

Training process

The algorithm used to adjust the weights for both subnetworks NI and NC is the generalized dynamic backpropagation algorithm (GDBPA) developed in the next section.

Offline training of the neuro-identifier

Training process is accomplished by switching on the neuro-identifier (NI) to operate in parallel with the synchronous generator, which is controlled by a conventional excitation control system [17], named (CECS). Small random signals are included as noise to the reference voltage. The differences between the respective outputs of the turbogenerator model (U_g,P_g) and the outputs of NI (U_g^*,P_g^*) generate the error signals for updating the NI weights which initially were set to small random values. The offline training is stopped when the mean square error between the identified output signals (U_g^*,P_g^*) and the actual plant output signals (U_g,P_g) reaches a small number (in this case 0.0001). The identifier training is usually achieved after 1250 s training.

Offline training of the neuro-controller

For the neuro-controller (NC) offline training, a conventional AVR with PSS is used to control the plant. The plant output signals (U_g,P_g) fed to the neuro-controller with the previous two values. The NC output u is compared to the conventional excitation control system (CECS) output. The deviation between the two signals is used to update the neuro-controller weights. The NC training has been performed for various load conditions and disturbances. The weights are adjusted till the mean square error obtained has been reduced to a minimum value of 0.0001.

Online training of the neuro-identifier and the neuro-controller

When the offline trainings of the neuro-identifier NI and the neuro-controller NC are terminated, these two subnetworks are switched on to replace the conventional excitation control system (CECS): the NI is used to learn the plant dynamics and the NC to control the plant. The online training of the subnetworks is illustrated in figure 1. The error between the plant output signal and the neuro-identifier output signal is propagated to adjust the NI weights. The error between the desired values of plant output and the neuro-identifier output is used to update the NC weights.

In this paper, three types of neural networks are separately considered, to design the neural network based excitation control system: a feedforward neural network (FFNN), a first-order diagonal recurrent neural network (1_DRNN) and a second-order diagonal recurrent neural network (2_DRNN). The structures of these networks are presented in figures 2, 3 and 4.

Generalized dynamic backpropagation algorithm for diagonal recurrent neural network training

The mathematical model for the second-order diagonal recurrent network (2_DRNN) of figure 4 is as follow:

$$u(k) = \sum_{j=1}^{q} w_j^u Z_j \tag{2}$$

(3) $$Z_j = \sigma(S_j(k))$$

(4) $$S_j(k) = w_j^{D1} Z_j(k-1) + w_j^{D2} Z_j(k-2) + \sum_{i=1}^{p} w_{ij}^{e} E_i(k)$$

where for each discrete time k, $E_i(k)$ is the *i-th* input to the DRNN, $S_j(k)$ is the sum of inputs to *j-th* recurrent neuron, $Z_j(k)$ is the output of the *j-th* recurrent neuron, and $u(k)$ is the output of the DRNN. w^e, w^{D1}, w^{D2} and w^u are respectively input, first-order recurrent, second-order recurrent and output weight vectors. $\sigma(.)$ is the sigmoid function given in equation (1).

Let y_d and $y(k)$ be the desired and the real plant output respectively. The error cost function is defined by

(5) $$J(k) = \frac{1}{2}(y_d - y(k))^2$$

The gradient of error in equation (5) with respect to an arbitrary weight vector $w \in \mathrm{R}^n$ is represented by:

(6) $$\frac{\partial J}{\partial w} = \frac{\partial}{\partial w}\left[\frac{1}{2}(y_d - y(k))^2\right] = -\Delta y(k)\frac{\partial y(k)}{\partial u(k)}\frac{\partial u(k)}{\partial w}$$

where $\Delta y(k) = y_d - y(k)$ is the error between the desired value and the output of the plant. The factor $\partial y(k)/\partial u(k)$ represents the sensitivity of the plant with respect to its input.

The output gradient $\partial u(k)/\partial w$ needs to be computed for both NI and NC. Its computation is summarized as follows. The output gradients with respect to output, recurrent, and inputs weights, respectively, are given by:

(7) $$\frac{\partial u(k)}{\partial w_j^u} = Z_j(k)$$

(8) $$\frac{\partial u(k)}{\partial w_j^{D1}} = w_j^u \frac{\partial Z_j(k)}{\partial w_j^{D1}}$$

(9) $$\frac{\partial u(k)}{\partial w_j^{D2}} = w_j^u \frac{\partial Z_j(k)}{\partial w_j^{D2}}$$

(10) $$\frac{\partial u(k)}{\partial w_{ij}^{e}} = w_j^u \frac{\partial Z_j(k)}{\partial w_{ij}^{e}}$$

Let

(11) $$P_{ij}(k) = \frac{\partial Z_j(k)}{\partial w_j^{Di}}$$

and

(12) $$Q_{ij}(k) = \frac{\partial Z_j(k)}{\partial w_{ij}^{e}}$$

Then:

(13) $$P_{ij}(k) = \frac{\partial Z_j(k)}{\partial S_j(k)}\frac{\partial S_j(k)}{\partial w_j^{Di}} = \sigma'(S_j(k))\frac{\partial S_j(k)}{\partial w_j^{Di}}$$

$$= \sigma'(S_j(k))\frac{\partial}{\partial w_j^{Di}}\left[\sum_{l=1}^{p} w_{lj}^{e} E_l + \sum_{m=1}^{2} w_j^{Dm} Z_j(k-m)\right]$$

$$= \sigma'(S_j(k))\left[Z_j(k-i) + \sum_{m=1}^{2} w_j^{Dm}\frac{\partial Z_j(k-m)}{\partial w_j^{Di}}\right]$$

$$= \sigma'(S_j(k))\left[Z_j(k-i) + \sum_{m=1}^{2} w_j^{Dm} P_{ij}(k-m)\right]$$

(14) $$Q_{ij}(k) = \sigma'(S_j(k))\frac{\partial S_j(k)}{\partial w_{ij}^{e}}$$

$$= \sigma'(S_j(k))\frac{\partial\left[\sum_{l=1}^{p} w_{lj}^{e} E_l + \sum_{m=1}^{2} w_j^{Dm} Z_j(k-m)\right]}{\partial w_{ij}^{e}}$$

$$= \sigma'(S_j(k))\left[E_i + \sum_{m=1}^{2} w_j^{Dm}\frac{\partial Z_j(k-m)}{\partial w_{ij}^{e}}\right]$$

$$= \sigma'(S_j(k))\left[E_i + \sum_{m=1}^{2} w_j^{Dm} Q_{ij}(k-m)\right]$$

where $\sigma'(.)$ is the derivative of the function $\sigma(.)$ defined in equation (1).

To calculate $P_{ij}(k)$ and $Q_{ij}(k)$ we suppose the following initial values:

(15) $$P_{ij}(0)=0,\ P_{ij}(1)=0,$$

(16) $$Q_{ij}(0)=0,\ Q_{ij}(1)=0.$$

Therefore, the weights are adjusted by the following equation:

(17) $$w(k+1) = w(k) + \eta\left(-\frac{\partial J(k)}{\partial w(k)}\right)$$

where η represents the learning rate whose the value is determined empirically so that a compromise between the training time and the accuracy of the network is achieved.

The above algorithm can be used not only to adjust the DRNN weights but also to adjust the FFNN weights. In the case of FFNN all the weight vectors w^{D1} and w^{D2} must be equal zero.

Simulation tests

In order to evaluate and compare effectiveness of each previously described neural controllers (FFNN, 1_DRNN, 2_DRNN), simulation tests have been carried out for the single machine infinite bus power system of figure 5. This system consists of a three-stage turbine that provides a mechanical power, a synchronous generator that transforms mechanical power in an electrical active power P_g and a reactive power Q_g and provides an output voltage U_g. The generator is connected to an infinite bus system through a step-up transformer and parallel transmission lines. The differential equations and parameters used to simulate the dynamic behavior of the synchronous generator are presented in Appendix A1. However, the mathematical models of the governor and turbine, of the conventional automatic voltage regulator (AVR) with PSS and excitation system are given in [17].

In the performed simulation tests different loading conditions and disturbances have been considered. Due to limited space, only the results for loading condition P_g=0,8 in p.u. and Q_g=0,2 in p.u., with a leading power factor, are

presented in this paper. The applied disturbances are as follows:

- 5% step increase at *t*=0s and 5% step decrease at *t*=5s in the infinite bus voltage;
- three phase short circuit at *t*=0s and cleared 200ms later;
- 20% step decrease in the reference power.

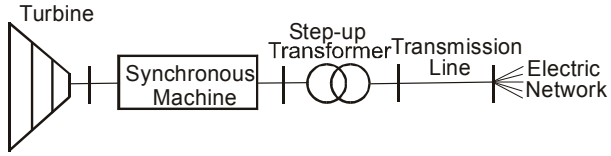

Fig. 5. Schematic diagram of the power system model

The results with each disturbance are depicted in figures 6÷11. Figures 6, 7 and 8 show the responses of the turbo-generator unit with each of the considered neural networks: FFNN, 1_DRNN and 2_DRNN. In each figure, terminal voltage variations and angular speed variations are presented. The responses with diagonal recurrent neural networks are indicated by solid lines of different thickness and those with feedforward neural network by dashed lines.

Figure 6 shows system responses to ±5% step changes in infinite bus voltage, figure 7 the system responses to three phase short circuit and figure 8 the system responses to 20% step decrease in reference power.

It can be seen from figure 6 that the angular speed overshot during the first alternance is more damped with 2_DRNN than with 1_DRNN and FFNN. Therefore the voltage overshot during this period is a little bit higher with 2_DRNN than with the two other neural networks. Figure 7 shows clearly that the voltage control and the damping of angular speed oscillations with 2_DRNN and with 1_DRNN are much better than with FFNN. In this case the damping with 2_DRNN is even slightly higher than with 1_DRNN. In figure 8 the voltage overshot and the angular speed overshot with 2_DRNN are more damped that with the two other neural networks.

The described above simulation results show that the proposed 2_DRNN is more efficient comparatively to 1_DRNN and to FFNN. To confirm the superiority of the proposed 2_DRNN, an additional study was performed: the performance of the 2_DRNN has been compared with the performance of IEEE 1S excitation control system with conventional PSS [17] designated by CECS. In this study, the same disturbances as previously were applied. The results with both control systems are illustrated in figures 9, 10 and 11. It show once again that the proposed 2_DRNN yields much better voltage control and much higher damping of electromechanical oscillations.

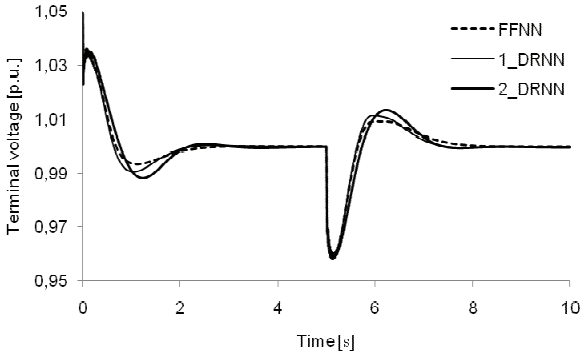

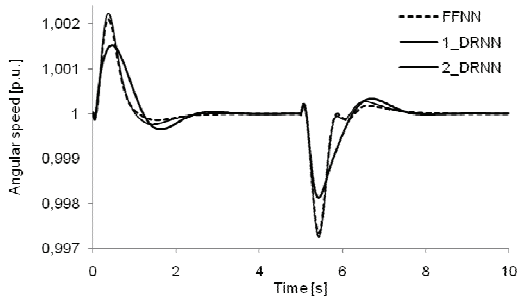

Fig. 6. Responses to step changes in infinite bus voltage

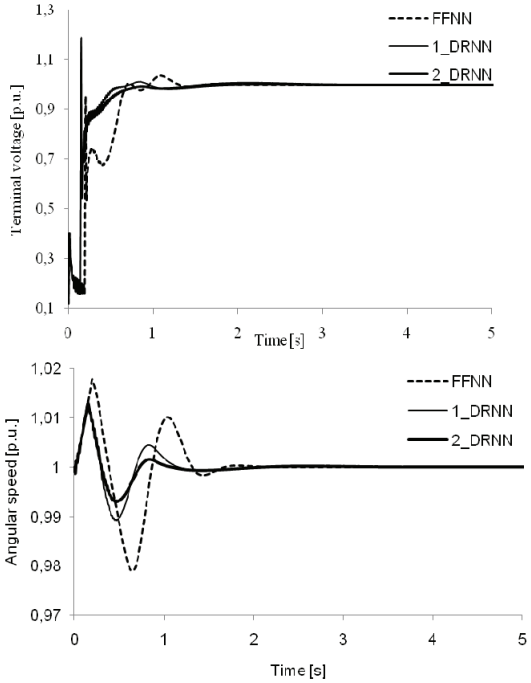

Fig. 7. Responses to three phase short circuit

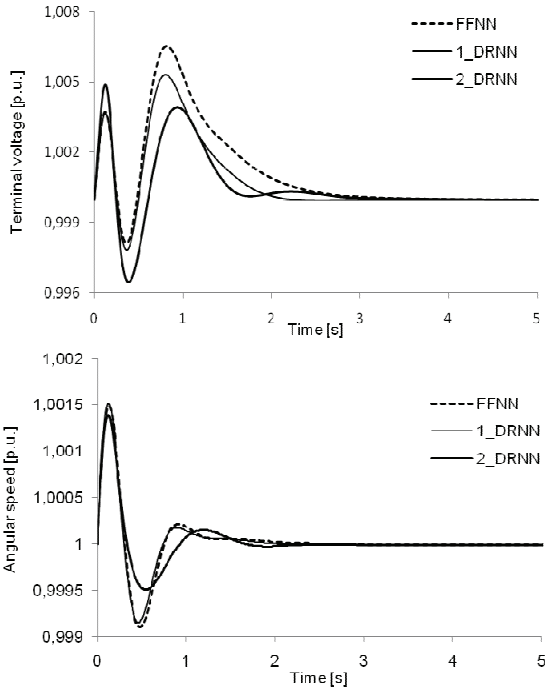

Fig. 8. Responses to step decrease in reference power

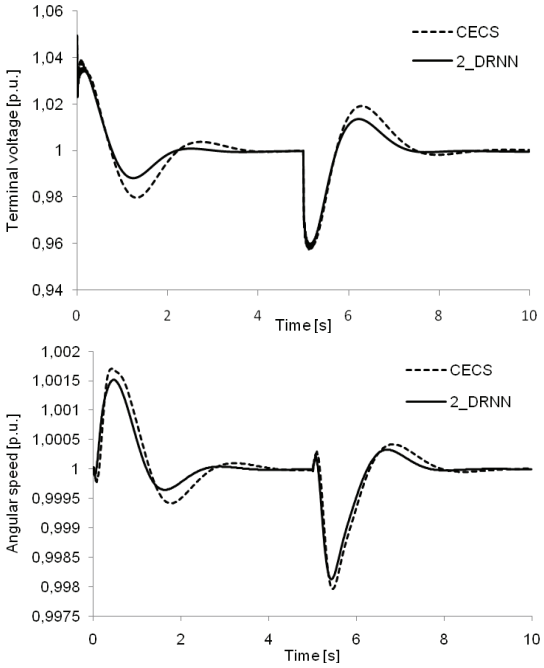

Fig. 9. Responses to step changes in infinite bus voltage

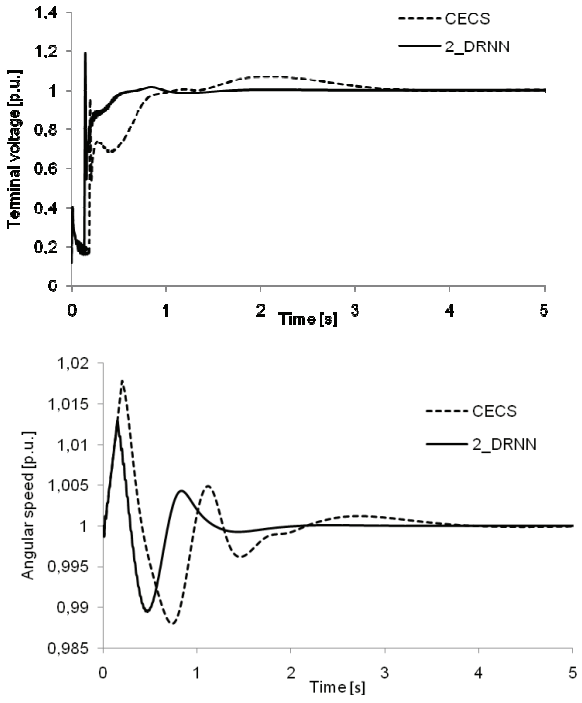

Fig. 10. Responses to three phase short circuit

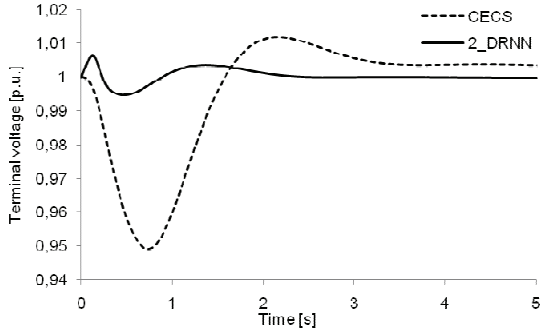

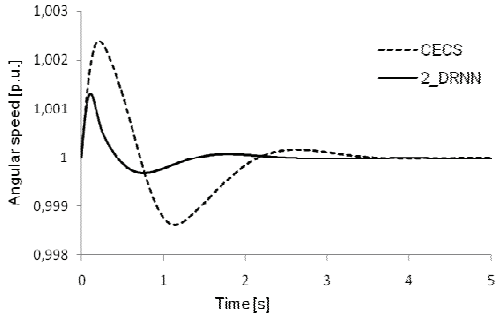

11. Responses to step decrease in reference power

Conclusion

In this paper three types of neural networks, used for modeling and control of turbogenerator unit connected to an infinite bus power system, have been investigated. These neural networks are: the Feedforward Neural Network (FFNN), the first-order Diagonal Recurrent Neural Network (1_DRNN) and the proposed second-order Diagonal Recurrent Neural Network (2_DRNN). Each of the neural networks has first been subjected to an offline training process using the generalized dynamic backpropagation algorithm (GDBPA) developed in this paper. Once the training process terminated, the neural network has been switched on to replace the conventional excitation control system with PSS.

The performances of the neural networks have been evaluated through simulation tests, under various operating conditions and disturbances. The test results have been compared and the proposed 2_DRNN has proved to be more efficient. Moreover, to confirm the superiority of the 2_DRNN, its dynamic and transient operation was also compared to the operation of the IEEE conventional excitation control system (CECS). Here also, the 2_DRNN beats the CECS in terms of offering better voltage control and better damping of electromechanical oscillations.

Moreover, it is important to mention that the proposed 2_DRNN performs two functions simultaneously: that of Automatic Voltage Controller (AVR) and that of Power System Stabilizer (PSS). Its architecture is very simple.

REFERENCES

[1] Mohammadzaheri M., Member L.C.: A design approach for feedback-feedforward control systems, *American Control Conference (ACC)*, 2010.

[2] Ting-Li C., Chung-Cheng C., Yi-Chieh H., Wen-Jiun L.: Stability and almost disturbance decoupling analysis of nonlinear system subject to feedback linearization and feedforward neural network controller, *Neural Networks, IEEE Transactions on*, volume 19, 2008.

[3] Min H.,; Wei G., Jincheng W.: Predictive control based on feedforward neural network for strong nonlinear system, *Neural Networks, 2005 IJCNN'05, Proceedings, 2005 IEEE Internationa Joint Conference,* Volume 4, 2005, 2266÷2271.

[4] Parisini T., Zoppoli R.: Neural networks for feedback feedforward nonlinear control systems, *Neural Networks, IEEE Transactions on*, Volume 5, issue 3, 1994,436÷449.

[5] Kuschewski, J.G., Hui, S., Zak S.H.: Application of feedforward neural networks to dynamical system identification and control, *Control Systems Technology, IEEE Transactions on*, Volume 1, Issue 1, 1993, 37÷49.

[6] Thomas R.J., Sakk E.: On using an artificial feedforward neural network as a controller in large –scale power systems, *Circuits and Systems, IEEE International Symposium on,* vol. 2, 1991, 1133-1136.

[7] Tiliouine H.: A modified neural network controller configuration, *14th International Conference on Methods and Models in Automation and Robotics, Międzyzdroje*, Poland, Volume 14, part I, August 2009.

[8] Sumina, D., Bulic, N., Erceg, G.: Simulation model of neural network based synchronous generator excitation control, *Power Electronics and Motion Control Conference, 2008. EPE-PEMC 2008. 13th*, 556-560.
[9] Venayagamoorthy G.K., Harley R.G.: A continually online trained neuro-controller for excitation and turbine control of a turbogenerator, *IEEE Transactions on Energy Conversion, 16 (16),* 2001, 261÷269.
[10] Salem M.M, Zaki A.M., Mahgoub O.A., Abu El_Zahab E., Malik O.P.: Studies on a multi-machine power system with a neural network based excitation controller, *Power Engineering Society Summer Meeting, 2000 IEEE*, Volume 1, 105 ÷ 110.
[11] Lubośny Z.: Adaptacyjny neuronowy regulator generator synchronicznego, *Przegląd Elektrotechniki R.80*, nr 10, 2004, 971÷974,.
[12] Chun-Jung C., Tien-Chi C., Hung-Jung H. and Chin-Chih O.: PSS design using adaptive recurrent neural network controller, *Fifth International Conference on Natural Computation,* Volume 2, 2009, 277÷281.
[13] Yingyi J., Chengli S.: Adaptive model predictive control using diagonal recurrent neural network, *Natural Computation*, *ICNC '08. Fourth International Conference on*, Volume 2, 2008, 276÷280.
[14] Xiaochen H., Yen, G.G.: Local signal based supplementary excitation controller for damping inter-area oscillations through recurrent neural networks, *Neural Networks, IJCNN 2007. International Joint Conference on*, 2007, 2498÷ 2503.
[15] Jeen-Shing W., Yen-Ping C.: A fully automated recurrent neural network for unknown dynamic system identification and control. *Circuits and Systems I: Regular Papers*, *IEEE Transactions on*, Volume 53, 2006, 1363÷1372.
[16] Chi-Huang L., Ching-Chih T.: Design and experimental evaluation of an adaptive predictive controller using recurrent neural network, *Systems, Man and Cybernetics*, *2005 IEEE International Conference on*, Volume 1, 2005, 690÷695.
[17] IEEE Recommended practice for excitation system models for power system stability studies, *IEEE Std 421.5-2005 (Revision of IEEE Std 421.5-1992),* 2006, 1÷85.

A.1. Differential equations of synchronous generator

$$\frac{1}{\omega_S}\frac{d\psi_d}{dt} = -u_d - \omega\psi_q - r_s i_d \tag{18}$$

$$\frac{1}{\omega_S}\frac{d\psi_q}{dt} = -u_q + \omega\psi_d - r_s i_q \tag{19}$$

$$\frac{1}{\omega_S}\frac{d\psi_f}{dt} = u_f - r_f i_f \tag{20}$$

$$\frac{1}{\omega_S}\frac{d\psi_{kd}}{dt} = -r_{kd} i_{kd} \tag{21}$$

$$\frac{1}{\omega_S}\frac{d\psi_{kq}}{dt} = -r_{kq} i_{kq} \tag{22}$$

$$\frac{1}{\omega_S}\frac{d\delta}{dt} = \omega - 1 \tag{23}$$

$$\frac{d\omega}{dt} = \frac{1}{2H}(T_m - T_e) \tag{24}$$

A.2. Nomenclature

ψ_d, ψ_q flux linkage in d q axis

ψ_f field flux linkage

ψ_{kd}, ψ_{kq} damping flux linkage in d q axis

u_d, u_q generator voltage in d q axis

i_d, i_q generator current in d q axis

u_f field voltage

$\mathrm{i_{kd}}, \mathrm{i_{kq}}$ damping current in d q axis

r_{kd}, r_{kq} damping windings resistance in d q axis

S_n rated apparent power
P_n rated active power
U_n rated voltage
I_n rated current
$cos\varphi_n$ rated power factor

r_s stator windings resistance

x_s stator leakage reactance

x_d direct axis synchronous reactance

x_d' transient reactance in d axis

x_d'' subtransient reactance in d axis

x_q quadrature axis synchronous reactance

x_q'' subtransient reactance in q axis

T_d' transient time constant in d axis

T_d'' subtransient time constant in d axis

T_q'' subtransient time constant in q axis

T_m mechanical torque
T_m electrical torque
J moment of inertia
ω_s synchronous angular speed

Table 1. Synchronous generator parameters

S_n	426 MVA
P_n	360 MW
U_n	22 kV
I_n	11.18 kA
$cos\varphi_n$	0.85
r_s	0.00233 p.u.
x_s	0.199 p.u.
x_d	2.6 p.u.
x_d'	0.33 p.u.
x_d''	0.24 p.u.
x_q	2.48 p.u.
x_q''	0.25 p.u.
T_d'	1.1 s
T_d''	0.03 s
T_q''	0.03 s
ω_s	100π s^{-1}
J	32300 kgm^2

Author:
dr inż. Hocine Tiliouine, Politechnika Gdańska, Katedra Elektrotechniki Teoretycznej i Informatyki, ul. Narutowicza 11/12 80-233 Gdańsk, h.tiliouine@ely.pg.gda.pl.